IAC-22-B4.IP.50

Analysis of Sun-acquisition Magnetic Attitude Control for Nanosatellite Using a Hardware-in-the-loop Satellite Simulator

Renato Borges[a], Danil Ivanov[b]*, Yasmin Ferreira[c], Dmitry Roldugin[d], Mikhail Ovchinnikov[e], Guilherme Bertoldo Guerra[f], Matheus Arruda[g], Lukas Lorenz de Andrade[h], Emanuel Brenag[i]

[a] *University of Brasilia, Brazil*, raborges@aerospace.unb.br
[b] *Keldysh Institute of Applied Mathematics, RAS, Russian Federation*, danilivanovs@gmail.com
[c] *University of Brasilia, Brazil*, yasmin.frrcosta@gmail.com
[d] *Keldysh Institute of Applied Mathematics, RAS, Russian Federation*, rolduginds@gmail.com
[e] *Keldysh Institute of Applied Mathematics, RAS, Russian Federation*, ovchinni@keldysh.ru
[f] *University of Brasilia, Brazil*, uibertoldo@hotmail.com
[g] *University of Brasilia, Brazil*, matheus.leal133@gmail.com
[h] *University of Brasilia, Brazil*, ukaslorenzdeandrade@gmail.com
[i] *University of Brasilia, Brazil*, emanuelbrenag@gmail.com

* Corresponding Author

Abstract

In the framework of mutual project between the University of Brasilia and the Keldysh Institute of Applied Mathematics the Sun acquisition magnetic attitude control algorithm is developed and tested on the laboratory facility with Earth magnetic field imitator and nanosatellite mock-up suspended on the air-bearing test-bed. The main feature of the algorithm is that it does not require the Sun sensors, the direction to the Sun in body reference frame is calculated using magnetometer measurements processed by the extended Kalman filter and Sun direction model onboard. The developed control law is proportional to the unit Sun-direction derivative in the body reference frame. The calculated magnetic dipole is implemented by magnetorquers, the dipole interaction with local magnetic field provides the required control torque. As the result, the defined normal to the solar panels is aligned with the Sun direction and the satellite rotates around this axis. The main difference between the orbital motion and motion of the satellite mock-up is the disturbance torque due to inevitable shift between the suspension point and center of mass. The performance of the algorithm considering this difference is studied in the paper.
Keywords: CubeSat, attitude control, extended Kalman Filter, laboratory study

1. Introduction

Many nanosatellite missions based on CubeSats require special attitude motion according to demands of their payload. In some cases, there is no strict requirements on angular velocity or orientation of the satellite, that is why for satellites in LEO it is enough to use active magnetic attitude control system with minimal set of sensors for attitude motion determination [1]. Usually, it is used for angular velocity damping after the launch: onboard magnetorquers produce the magnetic dipole moment according to the well-known *Bdot* algorithm [2]. Afterwards, the satellite attitude motion is random, and it is determined by initial conditions and orbital disturbance torques. This random motion can lead to low effectiveness of solar panels due to high angles between the normal to the high-area side of the 3U CubeSat and Sun direction. It results in low power onboard that could be not enough for the payload. That is why for such a mission with low attitude motion requirements the magnetic control algorithm for Sun acquisition should be applied.

In the paper the proposed in [3,4] algorithm for Sun acquisition is tested in laboratory environment. The preliminary numerical simulation in [5] showed the possibility of experimental study of the algorithm even under the influence of the gravity torque due to shift of center of mass relative to the center of pressure. In the paper the results of laboratory experiments is presented and discussed.

2. Laboratory facility description

The laboratory facility LODESTAR is developed in University of Brasilia in the Laboratory of Simulation and Control of Aerospace Systems. It is presented in Fig. 1. It is consist of the geomagnetic field imitator based on three orthogonal pairs of Helmholtz coils able to produce magnetic induction of 140 000nT, air-bearing test-bed provided with compressed air for aircushion production and nanosatellite mock-up with autonomous attitude determination and control system.

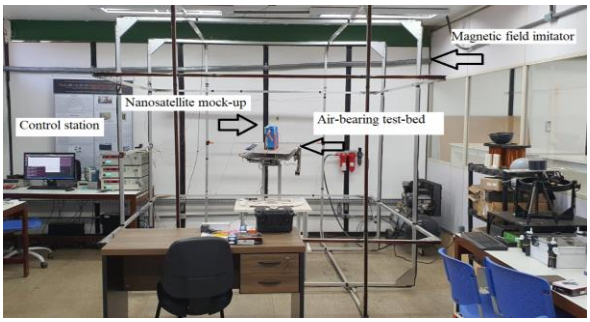

Fig. 1. Laboratory facility

The nanosatellite mock-up on the air-bearing test-bed is presented in Fig. 2. The platform with balancing system is placed on the air suspension and it is able to perform three-axis attitude motion – limitless along the vertical axis and constrained along the two horizontal axes. The mock-up in the form factor of 3U CubeSat is placed on the platform. The mock-up contains the onboard computer with implemented attitude determination and control algorithms. For attitude determination the measurement of onboard magnetometer are used. The angular velocity sensor measurements are not processed in the algorithms directly, but they used for angular velocity estimations validation. The onboard magnetorquers are able to produce the maximum magnetic dipole value of 0.34 Am^2 for the two coils and 0.39 Am^2 for a coil with a dipole directed along an elongated axis.

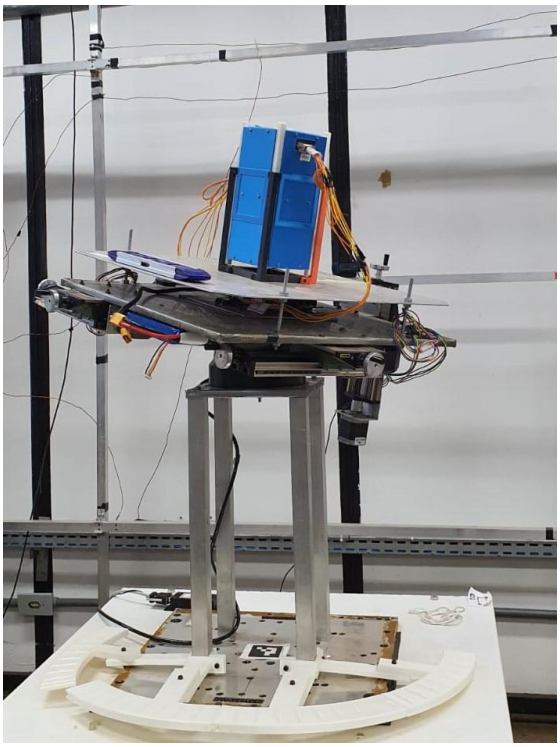
Fig. 2. Nanosatellite mock-up on air-bearing test-bed

The mock-up mass with the platform is 11.6 kg. Inertia tensor is $\mathbf{J}$ = (1.3, 1.7, 1.5) kg m^2.

3. Motion equations and control algorithm

Two reference frames are used:

- laboratory frame $OX_1X_2X_3$, here O is the mock up center of rotation, OX_3 is directed vertically;
- bound frame $Ox_1x_2x_3$, its axes coincide with the principal axes of inertia of the mock up.

Mock up attitude with respect to the laboratory frame is given by the Euler angles φ,ψ,θ (rotation sequence 3-1-3), angles α, β, γ (rotation sequence 2-3-1) and angular velocity components. Quaternion is used in the numerical simulation. The direction cosines matrix is given with expressions

$$\mathbf{A}=\begin{pmatrix} \cos\psi\cos\varphi-\sin\psi\cos\theta\sin\varphi & \sin\psi\cos\varphi+\cos\psi\cos\theta\sin\varphi & \sin\theta\sin\varphi \\ -\cos\psi\sin\varphi-\sin\psi\cos\theta\cos\varphi & -\sin\psi\sin\varphi+\cos\psi\cos\theta\cos\varphi & \sin\theta\cos\varphi \\ \sin\psi\sin\theta & -\cos\psi\sin\theta & \cos\theta \end{pmatrix} \quad (1)$$

and

$$\mathbf{A}=\begin{pmatrix} \cos\alpha\cos\beta & \sin\beta & -\sin\alpha\cos\beta \\ -\cos\alpha\sin\beta\cos\gamma+\sin\alpha\sin\gamma & \cos\beta\cos\gamma & \sin\alpha\sin\beta\cos\gamma+\cos\alpha\sin\gamma \\ \cos\alpha\sin\beta\sin\gamma+\sin\alpha\cos\gamma & -\cos\beta\sin\gamma & -\sin\alpha\sin\beta\sin\gamma+\cos\alpha\cos\gamma \end{pmatrix}$$

Dynamical equations of the mockup are

$$\mathbf{J}\frac{d\boldsymbol{\omega}}{dt}+\boldsymbol{\omega}\times\mathbf{J}\boldsymbol{\omega}=\mathbf{M}_{gr}+\mathbf{M}_{ctrl}+\mathbf{M}_{dist}, \quad (2)$$

$\mathbf{M}_{gr}$ is the gravitational torque, $\mathbf{M}_{ctrl}$ is the control magnetic torque, $\mathbf{M}_{dist}$ stands for any possible disturbances. Inertia tensor is given by

$$\mathbf{J}=\begin{pmatrix} I_{11}+mr_2^2+mr_3^2 & I_{12}-mr_1r_2 & I_{13}-mr_1r_3 \\ I_{12}-mr_1r_2 & I_{22}+mr_1^2+mr_3^2 & I_{23}-mr_2r_3 \\ I_{13}-mr_1r_3 & I_{23}-mr_2r_3 & I_{33}+mr_1^2+mr_2^2 \end{pmatrix}, \quad (3)$$

where I_{ij} are the inertia moments corresponding to the mockup center of mass, $\mathbf{r}$ is the vector connecting the center of rotation and the center of mass. Bound reference frame is often tied to the principal axes of inertia. In this case non diagonal terms I_{ij} vanish. The resulting inertia tensor $\mathbf{J}$ has non diagonal terms nevertheless due to the center of mass displacement. However, even loosely balanced mockup has quite small terms mr_ir_j. These are considered as disturbances and neglected for the analytical analysis. So the inertia tensor is diagonal. Numerical simulation implements proper inertia tensor according to (3). The torque arising from the gravity force is $\mathbf{M}_{gr}=-mg\mathbf{r}\times(a_{13},a_{23},a_{33})$.

Dynamical equations are supplemented with kinematics in angles

$$\frac{d\psi}{dt} = \frac{1}{\sin\theta}\left(\omega_1 \sin\varphi + \omega_2 \cos\varphi\right),$$
$$\frac{d\theta}{dt} = \omega_1 \cos\varphi - \omega_2 \sin\varphi, \quad (4)$$
$$\frac{d\varphi}{dt} = \omega_3 - \operatorname{ctg}\theta\left(\omega_1 \sin\varphi + \omega_2 \cos\varphi\right),$$

or

$$\frac{d\alpha}{dt} = \frac{1}{\cos\beta}\left(\Omega_2 \cos\gamma - \Omega_3 \sin\gamma\right),$$
$$\frac{d\beta}{dt} = \Omega_2 \sin\gamma + \Omega_3 \cos\gamma,$$
$$\frac{d\gamma}{dt} = \Omega_1 - \operatorname{tg}\beta\left(\Omega_2 \cos\gamma - \Omega_3 \sin\gamma\right).$$

Quaternion kinematics is used in numerical simulations.

The control torque for Sun-acquisition according to S-dot algorithm is as follows [6]:

$$\mathbf{M} = k\cos\alpha\left(\boldsymbol{\omega}\times\mathbf{S}\right)\times\mathbf{B}. \quad (5)$$

Here k is a positive control gain, $\mathbf{S}$ is the necessary direction of the third mockup axis in the laboratory frame, α is the angle between this direction and the magnetic induction vector. In case of the satellite, control (5) provides the alignment of the angular momentum vector along $\mathbf{S}$; alignment of the maximum moment of inertia axis along or opposite to the angular momentum vector; and rotation around this direction. For better understanding see Fig. 3.

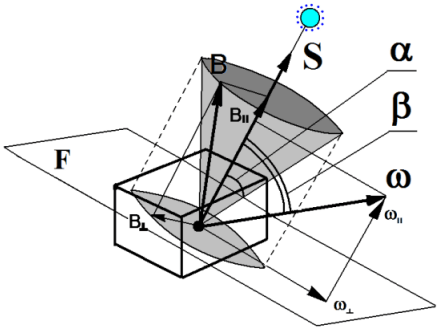

Fig. 3. Vectors direction in body reference frame

3. Attitude determination algorithm

In the experiment the magnetometer-only attitude motion determination is implemented using extended Kalman filter technique as in [1].

Kalman filter is a consistent recursive algorithm, that uses dynamic system model and sensors measurements to estimate system state vector. The vector estimation can be calculated for time moments $\hat{\mathbf{x}}_k = \hat{\mathbf{x}}(t_k)$ in case the measurements are discretely obtained at t_k moments. Discrete Kalman filter consist of two stages: prediction and correction.

Let the system be described by the following equations

$$\dot{\mathbf{x}}(t) = \mathbf{f}(\mathbf{x},t) + \mathbf{G}\mathbf{w}(t),$$
$$\mathbf{z}(t) = \mathbf{h}(\mathbf{x},t) + \mathbf{v}(t),$$

where $\mathbf{x}$ is the state vector, $\mathbf{z}$ is the measurements, $\mathbf{G}$ is weighting matrix, $\mathbf{w}, \mathbf{v}$ are the model and the measurements noises with corresponding covariance matrices $\mathbf{D}, \mathbf{R}$. We utilize extended Kalman Filter, so motion and measurements models must be linearized

$$\mathbf{H}_k = \left.\frac{\partial \mathbf{h}(\mathbf{x},t)}{\partial \mathbf{x}}\right|_{\mathbf{x}=\mathbf{x}_k^-,\, t=t_k}, \quad \mathbf{F}_k = \left.\frac{\partial \mathbf{f}(\mathbf{x},t)}{\partial \mathbf{x}}\right|_{\mathbf{x}=\mathbf{x}_k^-,\, t=t_k}.$$

Predicted parameters are obtained using

$$\mathbf{x}_k^- = \int_{t_{k-1}}^{t_k} \mathbf{f}(\mathbf{x}_{k-1}^+, t)dt;$$
$$\mathbf{P}_k^- = \boldsymbol{\Phi}_k \mathbf{P}_{k-1}^+ \boldsymbol{\Phi}_k^{\mathrm{T}} + \mathbf{Q}_k,$$
$$\mathbf{Q}_k = \int_{t_{k-1}}^{t_k} \boldsymbol{\Phi}_k \mathbf{G}\mathbf{D}\mathbf{G}^T \boldsymbol{\Phi}_k^T dt = \boldsymbol{\Phi}_k \mathbf{G}\mathbf{D}\mathbf{G}^T \boldsymbol{\Phi}_k^T \Delta t$$

where $\boldsymbol{\Phi}_k = \mathbf{E} + \mathbf{F}_k dt$, $\mathbf{P}$ is Kalman filter estimation covariance matrix. Corrected parameters are defined by

$$\mathbf{K}_k = \mathbf{P}_k^- \mathbf{H}_k^{\mathrm{T}} (\mathbf{H}_k \mathbf{P}_k^- \mathbf{H}_k^{\mathrm{T}} + \mathbf{R}_k)^{-1}$$
$$\mathbf{x}_k^+ = \mathbf{x}_k^- + \mathbf{K}_k [\mathbf{z}_k - \mathbf{h}(\mathbf{x}_k^-, t_k)]$$
$$\mathbf{P}_k^+ = [\mathbf{E} - \mathbf{K}_k \mathbf{H}_k] \mathbf{P}_k^-$$

The measurement models of magnetometer is as follows:

$$\mathbf{b}_{meas} = \mathbf{A}\mathbf{b}_{ECI} + \delta\mathbf{b},$$

where $\mathbf{A}$ is the transition matrix from orbital reference frame to body-fixed reference frame, $\mathbf{b}_{orb}$ is magnetic field vector in orbital reference frame, $\delta\mathbf{b}$ are Gaussian white noise with zero mean value.

In the paper state vector for Kalman filter consist of vector part of the quaternion, angular velocity vector and center of mass position relative to the suspension point

$$\mathbf{x} = \begin{bmatrix} \mathbf{q} \\ \boldsymbol{\omega} \\ \mathbf{r} \end{bmatrix}.$$

In this case the dynamical matrix is as follows [7]:

$$\mathbf{F}=\begin{pmatrix} -\mathbf{W}_{\boldsymbol{\omega}} & \frac{1}{2}\mathbf{E}_{3x3} & 0_{3x3} \\ \mathbf{J}^{-1}\mathbf{W}_{\mathbf{r}}\mathbf{W}_{mg} & \mathbf{J}^{-1}\mathbf{F}_{gyr} & -\mathbf{J}^{-1}\mathbf{W}_{mg} \\ 0_{3x3} & 0_{3x3} & 0_{3x3} \end{pmatrix},$$

where

$$\mathbf{F}_{gyr}=2\left(\mathbf{W}_{\mathbf{J}\boldsymbol{\omega}}\mathbf{W}_{\boldsymbol{\omega}}-\mathbf{W}_{\boldsymbol{\omega}}\mathbf{J}\mathbf{W}_{\boldsymbol{\omega}}\right),$$

$\mathbf{W}_{\mathbf{y}}$ is the skew-symmetric matrix filled by the components of vector $\mathbf{y}$.

The measurement matrix is as follows

$$\mathbf{H}=\begin{bmatrix}2\mathbf{W}_{\mathbf{b}} & 0_{3x3} & 0_{3x3}\end{bmatrix}.$$

4. Mock-up Motion Analysis

Planar horizontal motion is of utter importance even for the three dimensional experiments on the air bearing. Only rotation around the local vertical is not restricted while the rotation around the horizontal axis is always limited by about 30 degrees.

Consider the satellite moving on the polar orbit. Assume no gravity torque in (5), let $\alpha=\gamma=0$, $\omega_1=\omega_2=0$, and place vector $\mathbf{S}$ in the orbital plane. The planar motion equation is

$$\ddot{\beta}+\chi\dot{\beta}\left(\mathbf{B}\cdot\mathbf{S}\right)^2=0, \tag{6}$$

where $\chi=kB_0/C$ and the induction vector has unit length. The control torque (5) should be rewritten as

$$\mathbf{M}=k\left(\mathbf{B}\cdot\mathbf{S}\right)\left(-\boldsymbol{\omega}\left(\mathbf{B}\cdot\mathbf{S}\right)+\mathbf{S}\left(\mathbf{B}\cdot\boldsymbol{\omega}\right)\right). \tag{7}$$

So if $\mathbf{S}$ and $\mathbf{B}$ lie in the same plane this provides

$$\mathbf{M}=-k\left(\mathbf{B}\cdot\mathbf{S}\right)^2\boldsymbol{\omega}.$$

Suppose that Helmholtz coils provide the simplified geomagnetic field model in the laboratory frame,

$$\mathbf{B}=B_0\begin{pmatrix}-\sin\Theta\sin 2\omega_0 t\\ \sin\Theta\cos 2\omega_0 t\\ \cos\Theta\end{pmatrix}, \tag{8}$$

where ω_0 =10^{-3} s^{-1} is approximate orbital velocity for the 350 km orbit,

$$\operatorname{tg}\Theta=\frac{3\sin 2i}{2\left(1-3\sin^2 i+\sqrt{1+3\sin^2 i}\right)}.$$

The induction vector has constant length and moves uniformly on the circular cone. In this case (6) transforms to

$$\ddot{\beta}+\chi\cos^2 2t\dot{\beta}=0,$$

so

$$\dot{\beta}(t)=\dot{\beta}(0)\exp\left(-\frac{1}{2}\chi\left(t+\frac{1}{4}\sin t\right)\right).$$

Outright integration and final β expression are unavailable. Consider the constant magnetic induction vector lying in the horizontal plane. Equation (6) then provides

$$\beta(t)=\beta(0)-\dot{\beta}(0)\left(e^{-t/\chi}-1\right)/\chi. \tag{9}$$

Sdot control algorithm doesn't provide necessary mockup attitude in this case. However, it is possible to estimate the position that the mockup acquires. For the slightly unbalanced mockup (note that no gravitational torque was assumed above) result (9) provides only approximate estimate. Moreover, the motion itself is only close to the horizontal. Fig. 4 and 5 bring the numerical simulation results of the mockup motion close to the planar one.

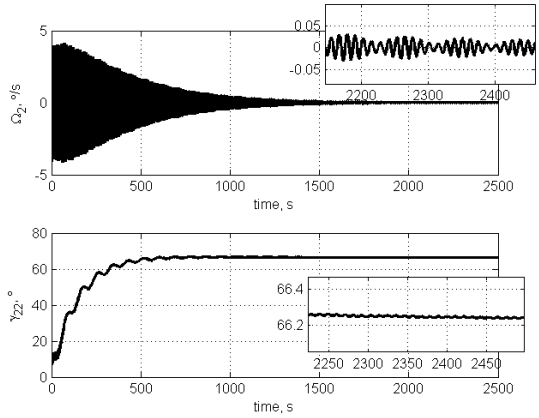

Fig. 4. Motion of the maximum moment of inertia (second) axis

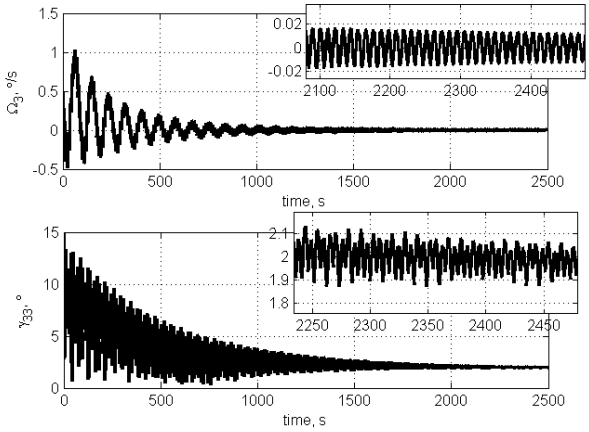

Fig. 5. Motion of the third mockup axis

Here γ_{ii} are the angles between the corresponding axes of reference frames. Initial conditions are $\alpha(0)=\gamma(0)=10$ °, $\beta(0)=6$ °, $\omega_1(0)=\omega_2(0)=0$, $\omega_3(0)=0.5$ °/s. Initial (without unbalance) inertia tensor is $\mathbf{I}=(1.3, 1.7, 1.5)$ kg·m^2, center of mass displacement is $\mathbf{r}=(0.1, 0, -3)$ mm, resulting control

gain $\chi = 1 \cdot 10^{-2}$ A·s/kg (control torque doesn't exceed 10^{-4} N·m, so for Helmholtz coils providing 150.000 nT field this corresponds to magnetorquers with dipole moment of about 1 A·m^2). Sdot control implementation ensures angular velocity damping. The mockup inclines by the angle of about 2° (equilibrium in the gravitational field corresponds to the inclination 1.9°) and rotates by the angle $\beta = 66°$. Note that the planar motion equation (9) assumes the rotation angle 80°. Relation (7) shows that the unwanted positional control part arises as the mockup deviates from the planar motion. The mockup tends to the position given by (9) until its angular velocity is damped.

Fig. 6 and 7 bring the same result for the center of mass deviation $\mathbf{r} = (1, 0, -3)$ mm (equilibrium corresponds to the inclination of about 18.4°).

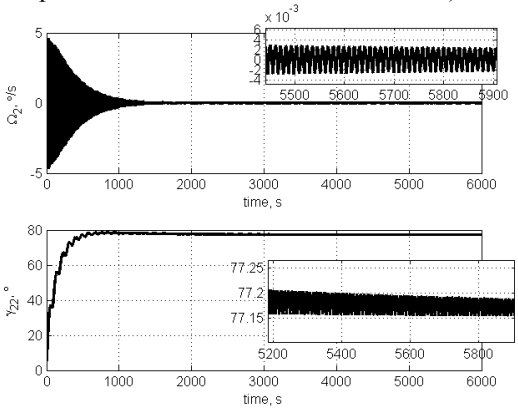

Fig. 6. Motion of the maximum moment of inertia axis

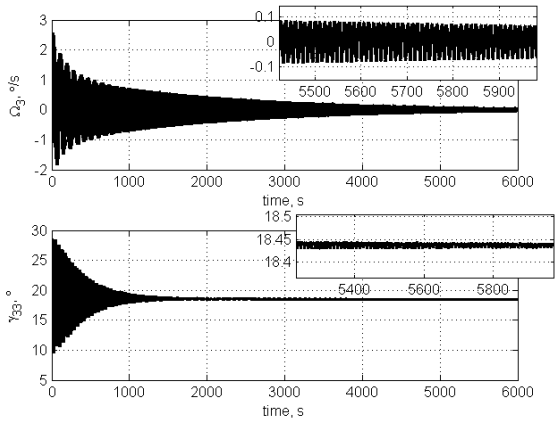

Fig. 7. Motion of the third mockup axis

To summarize, planar Sdot experiment allows very restricted algorithm verification. Angular velocity damping and rotation by the angle approximately given by (9) are anticipated.

5. Laboratory experiment results

The experiment to test the s-dot algorithm is as follows. Center of mass of the mock-up is shifted in vertical direction and in horizontal plane as well. The mock-up is provided with initial angular velocity. The magnetometer measurements are presented in Fig. 8.

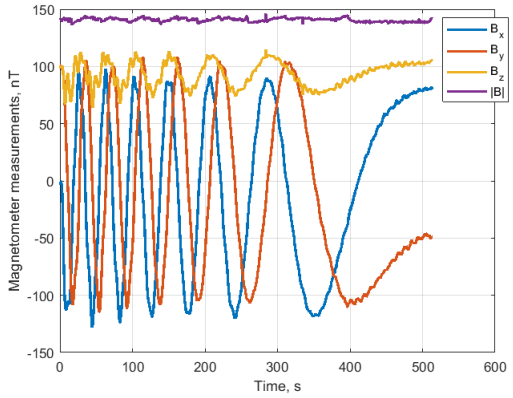

Fig. 8. Magnetometer measurements

The results of attitude quaternion and angular velocity estimation is presented in Fig. 9 and 10. The control values of magnetorquers are presented in Fig.11.

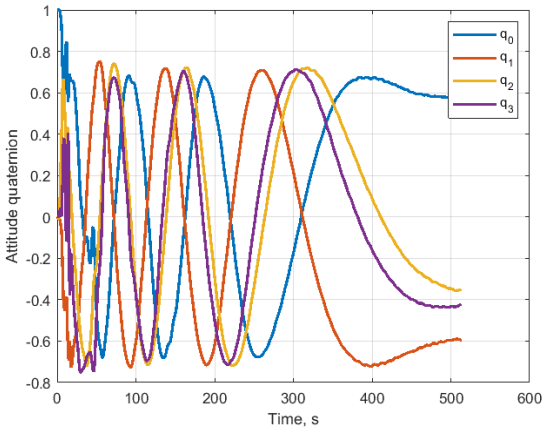

Fig. 9. Quaternion estimation

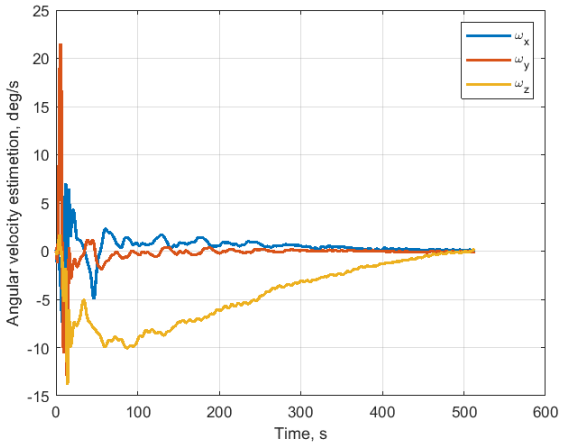

Fig. 10. Angular velocity estimation

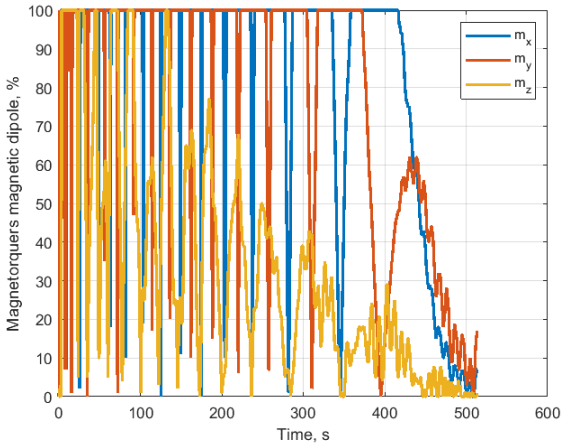

Fig. 11. Magnetoruqers magnetic dipoles

The nanosatellite mock-up is converged to the precession attitude motion after 500 seconds.

6. Conclusions

Despite on the difference in the external torques acting on the nanosatellite in orbit and on the mock-up on the air-bearing test-bed, the magnetic Sun-acquisition attitude control result in precession motion of the solar panels normal vectors around the Sun direction. Extended Kalman fitler based on magnetometer-only measurements is able to estimate the attitude motion of the mock-up in case the external magnetic field is not vertical. S-dot algorithm can be useful for nanosatellites power acquisition attitude control modes.

Acknowledgements

This work is partially supported by the Russian Science Foundation (sections 3 and 4 of the paper conducted by the Russian part), grant № 22-71-10009, and by the Brazilian National Council for Scientific and Technological (CNPq) and the Brazilian Federal District Research Support Foundation (FAPDF) (sections 1,2,5,6 of the paper conducted by the Brazilian part).

References

1. Ivanov, D.S.; Roldugin, D.S.; Tkachev, S.S.; Ovchinnikov, M.Y.; Zharkikh, R.; Kudryavtsev, A.; Bychek, M. Attitude motion and sensor bias estimation onboard the SiriusSat-1 nanosatellite using magnetometer only. *Acta Astronaut.* **2021**, *188*, 295–307, doi:10.1016/J.ACTAASTRO.2021.07.038.
2. Ovchinnikov, M.Y.; Penkov, V.I.; Roldugin, D.S.; Karpenko, S.O. Investigation of the effectiveness of an algorithm of active magnetic damping. *Cosm. Res.* **2012**, *50*, 170–176, doi:10.1134/S0010952512010078.
3. Roldugin, D.S.; Tkachev, S.S.; Ovchinnikov, M.Y. Satellite Angular Motion under the Action of SDOT Magnetic One Axis Sun Acquisition Algorithm. *Cosm. Res.* **2021**, *59*, 529–536, doi:10.1134/S0010952521100014/FIGURES/6.
4. Karpenko, S.O.; Ovchinnikov, M.Y.; Roldugin, D.S.; Tkachev, S.S. One-axis attitude of arbitrary satellite using magnetorquers only. *Cosm. Res.* **2013**, *51*, 478–484.
5. Ovchinnikov, M.Y.; Roldugin, D.S.; Borges, R.A.; Cappelletti, C.; Battistini, S. Modeling a Satellite Mockup's Angular Motion on an Air Bearing with Uniaxial Magnetic Attitude Control. *Math. Model. Comput. Simulations* **2020**, *12*, 474–481, doi:10.1134/S2070048220040146/FIGURES/8.
6. Ovchinnikov, M.Y.; Ivanov, D.S.; Ivlev, N.A.; Karpenko, S.O.; Roldugin, D.S.; Tkachev, S.S. Development, integrated investigation, laboratory and in-flight testing of Chibis-M microsatellite ADCS. *Acta Astronaut.* **2014**, *93*, doi:10.1016/j.actaastro.2013.06.030.
7. Ivanov, D.S.; Ivanova, T.A.; Ivlev, N.A.; Ovchinnikov, M.Y.; Roldugin, D.S. Estimation of an Inertia Tensor and Automatic Balancing of a Microsatellite Mockup on an Air-Bearing Testbed. *J. Comput. Syst. Sci. Int. 2021 602* **2021**, *60*, 315–332, doi:10.1134/S1064230721020088.